JACS
JOURNAL OF THE AMERICAN CHEMICAL SOCIETY

ARTICLE

pubs.acs.org/JACS

Reactions in the Rechargeable Lithium−O_2 Battery with Alkyl Carbonate Electrolytes

Stefan A. Freunberger,[†] Yuhui Chen,[†] Zhangquan Peng,[†] John M. Griffin,[†] Laurence J. Hardwick,[†] Fanny Bardé,[‡] Petr Novák,[§] and Peter G. Bruce*[,†]

[†]School of Chemistry, University of St. Andrews, North Haugh, St. Andrews, Fife KY16 9ST, U.K.

[‡]Toyota Motor Europe, Technical Centre, Hoge Wei 33 B, B-1930 Zaventem, Belgium

[§]Electrochemistry Laboratory, Paul Scherrer Institut, CH-5232 Villigen PSI, Switzerland

Supporting Information

ABSTRACT: The nonaqueous rechargeable lithium−O_2 battery containing an alkyl carbonate electrolyte discharges by formation of $C_3H_6(OCO_2Li)_2$, Li_2CO_3, HCO_2Li, CH_3CO_2Li, CO_2, and H_2O at the cathode, due to electrolyte decomposition. Charging involves oxidation of $C_3H_6(OCO_2Li)_2$, Li_2CO_3, HCO_2Li, CH_3CO_2Li accompanied by CO_2 and H_2O evolution. Mechanisms are proposed for the reactions on discharge and charge. The different pathways for discharge and charge are consistent with the widely observed voltage gap in Li−O_2 cells. Oxidation of $C_3H_6(OCO_2Li)_2$ involves terminal carbonate groups leaving behind the OC_3H_6O moiety that reacts to form a thick gel on the Li anode. Li_2CO_3, HCO_2Li, CH_3CO_2Li, and $C_3H_6(OCO_2Li)_2$ accumulate in the cathode on cycling correlating with capacity fading and cell failure. The latter is compounded by continuous consumption of the electrolyte on each discharge.

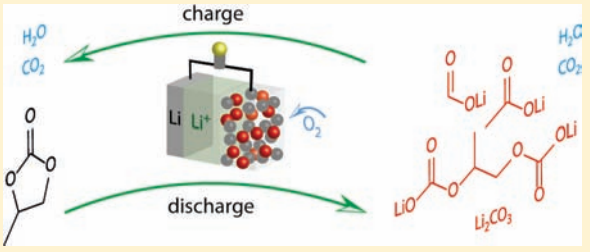

1. INTRODUCTION

The rechargeable lithium−O_2 battery is receiving a great deal of interest at the present time because, theoretically, it can store 5−10 times more energy than current lithium-ion batteries, the energy density of which can, at best, be doubled. The rechargeable lithium−O_2 battery could transform energy storage, vital in order to address global warming; however, it remains some way from a practical device at present.

The nonaqueous lithium−O_2 battery was first reported by Abraham and Jiang, with recent contributions by a number of groups, including those listed in the cited references.[1−18] A typical lithium−O_2 battery consists of a lithium anode, a Li^+ conducting organic electrolyte, and a porous cathode composed of carbon black, a catalyst, and binder.[1−4,8−10,17−27] It is believed that the Li−O_2 battery operates by reduction of O_2 (from the atmosphere) to form Li_2O_2 within the pores of the cathode, with the process being reversed on charge.[1−4,8−12,15−27]

Organic carbonate-based electrolytes (e.g., $LiPF_6$ in propylene carbonate) have been the most widely used in Li−O_2 cells to date.[1−4,8,10,17−22,24−26] However, recently it has been reported that such electrolytes decompose in Li−O_2 cells on discharge, rather than form Li_2O_2.[28−31] Despite such electrolyte decomposition, prototype Li−O_2 batteries with organic carbonate electrolytes have been described.[32] Organic carbonate cells have been shown to exhibit specific energies >1000 W h kg^{-1} (based on total mass of the electrode) and, in some cases, can sustain more than 100 cycles.[24,28] High capacity for a few 10 s of cycles may even be sufficient for some applications. Given the widespread use of organic carbonate electrolytes in Li−O_2 cells and their performance, it is important to understand the processes that occur on discharge and subsequent charge. What exactly are the discharge products? How do they form? How do they decompose on charging, and how does the cell cycle yet also fade and die? We show that on discharge a mixture of lithium propyl dicarbonate, $C_3H_6(OCO_2Li)_2$, Li_2CO_3, HCO_2Li, CH_3CO_2Li, CO_2, and H_2O is formed. Charging involves decomposition of $C_3H_6(OCO_2Li)_2$, HCO_2Li, CH_3CO_2Li, and Li_2CO_3 along with CO_2 and H_2O evolution. HCO_2Li, CH_3CO_2Li, Li_2CO_3, and $C_3H_6(OCO_2Li)_2$ accumulate in the cathode on cycling, correlating with capacity fading and cell failure alongside electrolyte consumption.

2. EXPERIMENTAL SECTION

2.1. Electrochemical Measurements. Propylene carbonate (PC) was distilled over a packed bed column and dried for several days over freshly activated molecular sieves (type 4 Å). All solvents had a final water content of ≤4 ppm (determined using a Mettler-Toledo Karl Fischer titration apparatus). Electrochemical grade $LiPF_6$ (Stella) was used for preparing the electrolytes. The electrochemical cells used to investigate cycling were based on a Swagelok design and composed of a Li metal anode, an electrolyte (1 M $LiPF_6$ in PC) impregnated into a glass fiber separator (Whatman), and a porous cathode. The porous cathode consisted of carbon black (Super P, TIMCAL), α-MnO_2

Received: March 9, 2011
Published: April 27, 2011

nanowires,[8] and polyvinylidenefluoride (PVdF-HFP, Kynarflex 2801) (mass ratios of 24:42:34) cast on glass from a slurry made with acetone. The cathodes used to explore charging of model compounds contained, in addition, the relevant finely ground compound. The cell was gastight except for the Al grid window that exposed the porous cathode to the O_2 atmosphere. The cell was operated in 1 atm of O_2. Electrochemical measurements were performed at room temperature using a Maccor battery cycler.

2.2. Synthesis. Model discharge compounds based on Li alkyl carbonate salts were synthesized by routes described in the Supporting Information.

2.3. Mass Spectrometry (MS). The cells again consisted of a lithium anode, electrolyte (1 M $LiPF_6$ in PC) impregnated into a glass fiber separator, and a porous cathode. MS analysis was carried out to examine the gases evolved on discharge and charge, by purging the cell with a carrier gas (N_2 or Ar) after charge or discharge, so that the gases evolved were transferred into the mass spectrometer. The process of charging Li_2CO_3 was followed by in situ differential electrochemical MS (DEMS) involving stepping the current while continuously flowing Ar to carry the gases evolved to the mass spectrometer. The experimental setup is described in detail elsewhere.[33]

2.4. Physical Characterization. All procedures were performed in an Ar-filled glovebox. Examination of electrodes involved first disassembling the cell; if not otherwise stated, rinsing the cathode twice with CH_3CN; and removing the solvent under vacuum. ^1H- and ^{13}C solid-state NMR experiments were performed on the cathode using a Bruker Avance III spectrometer operating at a magnetic field strength of 14.1 T. Experiments were performed using airtight rotors in a Bruker 2.5 mm probe, with a magic-angle spinning (MAS) rate of 30 kHz. For liquid-phase NMR analysis the previously rinsed and dried electrodes were extracted with D_2O, and then the extracted solution was examined on a Bruker Avance II 400 spectrometer. Spectra were referenced to the CH_3 peak of propylene glycol (found in the discharged electrodes) measured separately in $CDCl_3$. Powder X-ray diffraction (PXRD) was carried out using a STOE STADI/P diffractometer operating in transmission mode with a primary beam monochromator and position sensitive detector. Fe $K\alpha_1$ radiation (λ = 1.936 Å) was employed. The samples were contained in an airtight X-ray holder. FTIR measurements were carried out on a Nicolet 6700 spectrometer (Thermo Fisher Scientific) either in transmission with a CsI pellet or on an ATR unit in a N_2-filled glovebox.

2.5. In Situ Surface Enhanced Raman Spectroscopy (SERS). An electrochemical cell with a sapphire window was employed. The working electrode was exposed to an excitation wavelength of 632.8 nm using a Renishaw Raman system with collector optics based on a Leica inverted microscope.

3. RESULTS AND DISCUSSION

3.1. The Discharge Process. A typical Li−O_2 cell, consisting of a lithium metal anode, a 1 M solution of $LiPF_6$ in propylene carbonate as the electrolyte and a porous cathode (Super P/α-MnO_2/Kynar) was constructed as described in the Experimental Section. After galvanostatic discharge in O_2, the cell was disassembled, and FTIR data were collected from the cathode without exposure to air, Figure 1. The FTIR data extend down to 250 cm^{-1}, in order to include the spectral region within which the three bands of Li_2O_2 occur. Previous FTIR studies did not extend down to such low wavenumbers.[28,31] The FTIR spectrum in Figure 1 shows that the discharge products are not dominated by Li_2O_2, that there is a significant proportion of Li_2CO_3, and that peaks associated with C═O, C−O, C−C, and C−H groups are also present. In other words, the FTIR data demonstrate

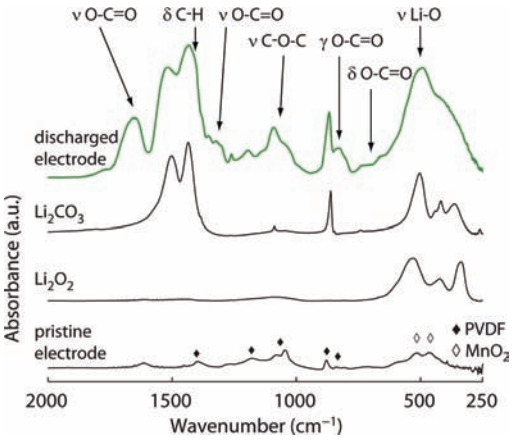

Figure 1. FTIR spectrum of a composite electrode (Super P/α-MnO_2/Kynar) discharged in 1 M $LiPF_6$/PC to 2 V in O_2. The reference spectra for Li_2O_2 (small impurity peaks at 1080, 1450, and 1620 cm^{-1}), Li_2CO_3, and the electrode before discharge are also shown.

severe decomposition of the organic carbonate electrolyte on discharge, in accord with recent studies.[28−31] It is worth noting that the presence of some electrolyte degradation is to be expected, based on studies of O_2 reduction in alkyl carbonates carried out some years ago.[34,35] The data in Figure 1 and in previous investigations were obtained on an electrode with a catalyst. To confirm that the electrolyte decomposition is not simply due to the catalyst, FTIR data were collected on glassy carbon and a porous electrode without a catalyst. The FTIR spectra at the end of discharge are shown in Figure S1 and confirm the dominance of electrolyte decomposition in the absence of catalyst.

Previous studies did not identify the specific discharge products that accompany Li_2CO_3; however, identifying such products is important in order to understand how the Li−O_2 cell operates in the absence of Li_2O_2 formation. Although FTIR spectroscopy has demonstrated decomposition and has identified the presence of Li_2CO_3, it is more difficult to distinguish between the other possible Li−organic products by FTIR alone. This is illustrated by examining the FTIR spectra of several possible discharge products. On discharge, O_2 is first reduced to O_2^-, which then attacks the PC and could, in principle, give rise to a variety of products. A number of these have been synthesized directly (as described in Supporting Information) and their spectra compared with those of the discharged cathode (see Figure S2). The spectra of some of these compounds are indistinguishable, e.g., f and g in Figure S2. Many of the spectra are too similar when present in a mixture with Li_2CO_3 and Kynar (as they are in the discharged electrode) to determine unambiguously which compounds form on discharge, Figure S2.

In order to make progress in identifying the specific discharge products, solid-state ^{13}C and ^1H NMR (ssNMR) data were collected on the discharged cathode, a and b of Figure 2, respectively; details of the NMR experiments are presented in the Experimental Section. The peak assignments are given in the figure. The spectra indicate the presence of several moieties, including carbonate, propyl, and H−C═O groups. While these results do give more insight into the nature of the products than FTIR, the ssNMR spectra alone cannot identify complete compounds. To address this problem the cathodes were washed with D_2O, and the resulting solution was subjected

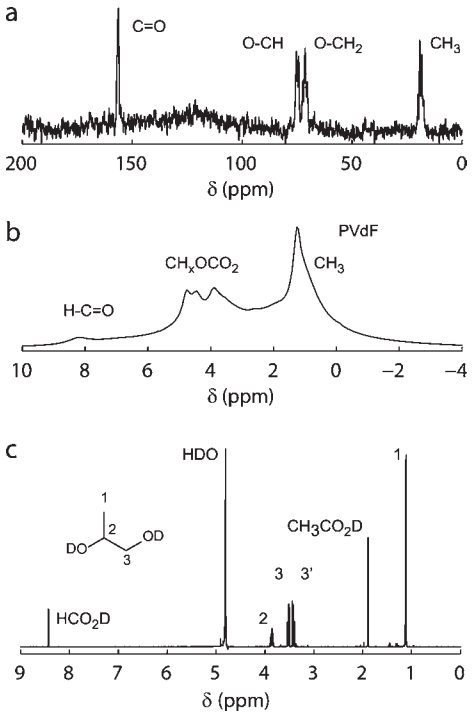

Figure 2. (a) ^{13}C MAS NMR spectrum of discharged composite electrode (Super P/α-MnO_2/Kynar). (b) ^{1}H MAS NMR spectrum of the same electrode. (c) ^{1}H solution NMR of the same electrode extracted with D_2O. Electrodes were discharged in 1 M $LiPF_6$/PC to 2 V under O_2.

to ^{1}H NMR spectroscopy. The spectrum is shown in Figure 2c and is consistent with the presence of propylene glycol, formic acid, acetic acid, and residual PC. Propylene glycol is the product expected from the reaction between Li propyl dicarbonate and water, according to the process $2ROCO_2Li + D_2O \rightarrow 2ROD + Li_2CO_3 + CO_2$. Similarly, formic and acetic acids arise from the reaction between Li formate, Li acetate, and D_2O. Integration of the areas under the peaks yields the following mole ratio of Li propyl dicarbonate/Li acetate/Li formate, 1:0.22:0.21 (corresponding to a mass ratio of 1:0.084:0.062). The presence of Li propyl dicarbonate, Li acetate, and Li formate in the discharged product is consistent with the ssNMR results and with the FTIR spectrum of the discharged electrode, Figure S3 (although, as stated above, it would have been difficult to identify all the discharge products from FTIR alone). Note that ^{1}H NMR of the electrolyte removed from the cell after discharge showed only PC, confirming that there are no discharge products in the liquid phase. The gases evolved on discharge were analyzed by MS (see Experimental Section) and shown to consist of H_2, H_2O, and CO_2, Figure S4. H_2 can arise by reaction of evolved H_2O with the Li metal anode. Therefore, combining all of the results, we have identified that the discharged product in the cathode contains Li propyl dicarbonate, Li_2CO_3, Li formate, and Li acetate and some residual PC trapped within the solid products as well as H_2O and CO_2.

Previous studies of reduction in Li^+−PC electrolytes have focused mainly on reactions aimed at understanding formation of the solid−electrolyte interface (SEI) layer on Li metal and graphite electrodes. As a result, such studies have taken place at much lower voltages than used here and in the absence of O_2; therefore, the mechanisms are not applicable to the present work.[36,37] Mechanisms have been proposed previously for the reaction between reduced O_2 species and PC.[34,38] Those in the absence of Li^+ cannot, of course, reproduce the products observed here. Some reports have suggested that in the presence of Li^+ reduced oxygen species lead to the formation of compounds containing alkoxy and carbonate groups.[34,38] In summary, none of the mechanisms proposed previously can explain the range of products observed here. To address this, we propose a possible reaction path in Scheme 1. For clarity we shall describe the scheme in three parts.

(i) The reactions on discharge commence with O_2 reduction to O_2^-. Early work regarding the reactivity of O_2^- toward esters suggested attack on the C of the carbonyl.[35,39] More recently, a DFT study on the nucleophilic attack of O_2^- on PC reported a prohibitively high activation energy for attack at this position, whereas attack at the CH_2 group via a S_N2 mechanism is much more favorable, in accord with earlier experimental studies.[40,41] Such a S_N2 addition of O_2^- to the methylene group, reactions 2 and 3 in Scheme 1, results in ring-opening and the formation of the peroxoradical species **2**. This then loses O_2, reaction 4, to form the bifunctional Li alkoxycarbonate radical **3**, which is easily reduced to form, in the presence of CO_2, the final product, Li propylene dicarbonate **4**.[42] Reaction 4 proceeds via a dimer of **2**.[43,44] Note that the CO_2 is generated by the reactions described in (ii), and its presence was demonstrated by MS analysis on discharge, Figure S4.

(ii) Intermediate **2** is known, in the presence of O_2, to easily undergo oxidative decomposition reactions.[44−46] There are many possible reaction pathways; in modeling such oxidative decomposition reactions (e.g., combustion reactions) 100 s of pathways are often considered, which makes it virtually impossible to formulate a unique reaction path.[44] Incomplete decomposition leads to the formation of formic and acetic acids. In the environment of the Li^+ electrolyte the equivalents are Li formate and Li acetate, which were observed as decomposition products in our studies.

(iii) Finally, formation of Li_2CO_3 can occur by reaction between O_2^- and CO_2, see reactions 6 and 7 in Scheme 1.[47,48] In addition to the mechanism shown in Scheme 1, H_2O formed in the oxidative decomposition reactions and was observed in MS analysis (Figure S4) and can react with the Li propylene dicarbonate to form Li_2CO_3, CO_2, and the corresponding alcohol.

The proposed reaction mechanisms are consistent with the discharge products observed by NMR, FTIR, and MS: $C_3H_6(OCO_2Li)_2$, Li_2CO_3, HCO_2Li, CH_3CO_2Li, CO_2 and H_2O.

Prior to the introduction of the nonaqueous Li−O_2 cell, several authors reported that organic carbonates and esters are susceptible to attack by reduced O_2 species,[35,36,39] yet it was widely believed that operation of the Li−O_2 cell in such electrolytes was dominated by Li_2O_2 formation on discharge. This was in part due to the cell's ability to sustain charge−discharge cycling and because of ex situ Raman spectra on a cathode after discharge, which showed evidence of Li_2O_2.[1] In contrast, recent reports based on FTIR and MS concluded that Li_2O_2 is not formed.[28,31] However, as shown in the FTIR spectrum of the discharged cathode in Figure 1 (extended down to 250 cm^{-1}), FTIR can clearly demonstrate extensive electrolyte decomposition, but it cannot rule out the formation of a

Scheme 1. Proposed Reaction Scheme on Discharge To Explain Formation of the Compounds: Li Propyl Dicarbonate, Li Formate, Li Acetate, Li_2CO_3, CO_2, and H_2O[a]

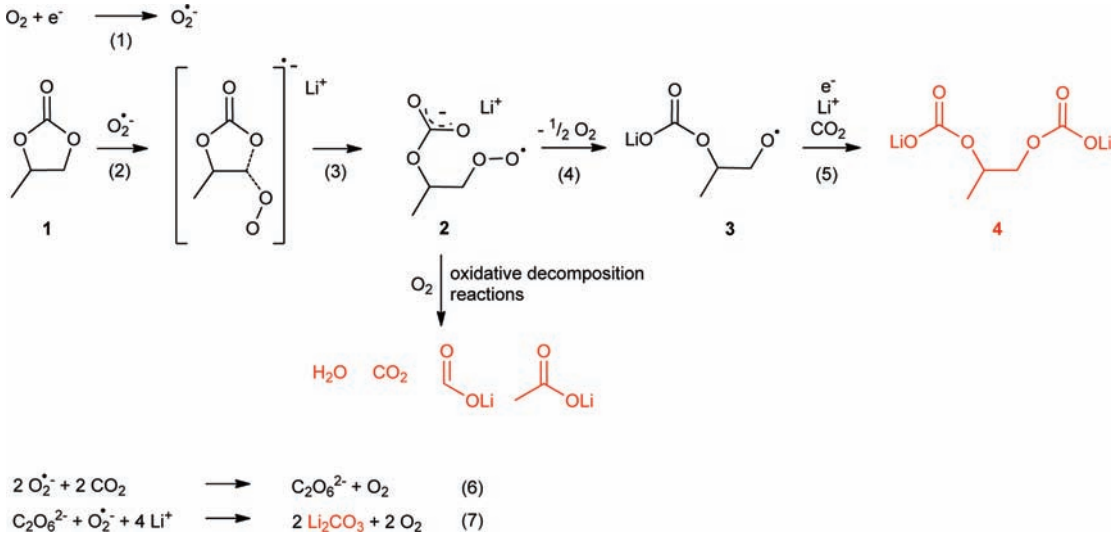

[a] The O_2^- generated in the first step could combine rapidly with Li^+, forming LiO_2, which may act as a nucleophile instead of, or as well as, O_2^-. The subsequent reactions in the scheme would be the same. However, no LiO_2 was detected on discharge by surface-enhanced Raman spectroscopy (SERS) in Figure 3.

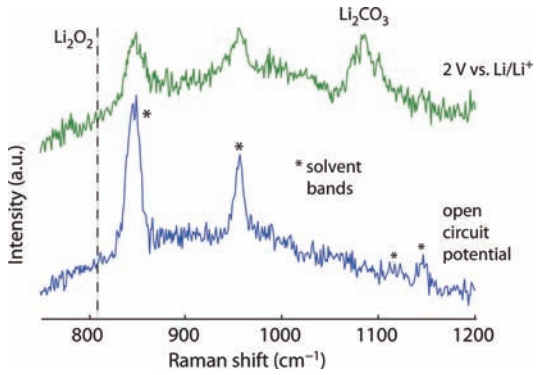

Figure 3. SERS on an Au electrode in 1 M $LiPF_6$/PC under O_2 at open circuit potential and after discharge to 2 V. The dashed line marks the position where Li_2O_2, if present, would occur.

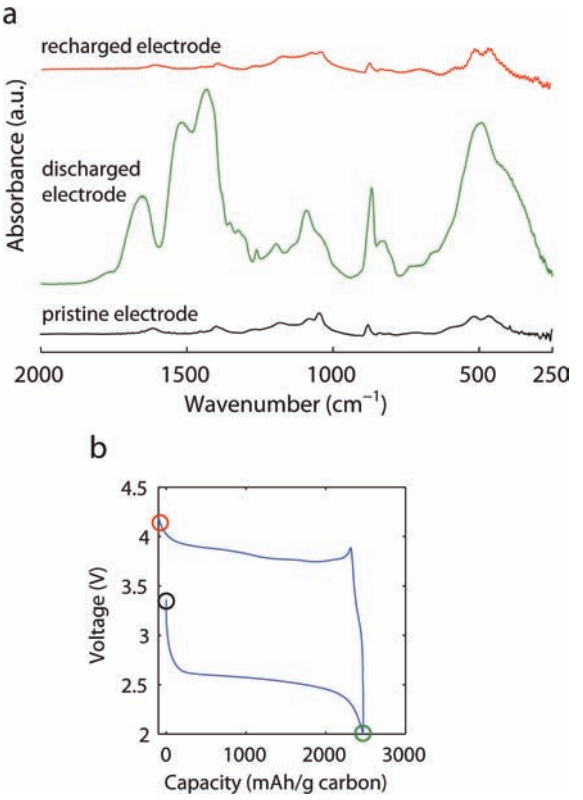

Figure 4. (a) FTIR spectra of a pristine electrode (Super P/α-MnO_2/Kynar) and after the first discharge, then charge in 1 M $LiPF_6$ in PC under O_2. (b) Variation of voltage as cell is discharged then charged.

minor amount of Li_2O_2 because of extensive overlap in the region of the three Li_2O_2 peaks with peaks from Li_2CO_3 and the other Li−organic compounds. The previous MS studies were carried out on charging a discharged electrode in He; it was concluded that Li_2O_2 was not formed on the basis of the absence of O_2 in the gases evolved on charging. These are excellent studies; however, we now know (see discussion in the next section) that charging the discharge products can involve reaction with O_2 so that, if Li_2O_2 had formed on discharge, the O_2 evolved on subsequent charging may have been consumed by oxidation of the Li−organic compounds. In view of the conflicting reports concerning the possible presence of Li_2O_2, we carried out in situ surface-enhanced Raman spectroscopy (SERS). Raman is particularly sensitive to Li_2O_2, and the in situ nature of the experiment ensures no contamination from air. SERS data collected at 2 V on a roughened Au electrode at the end of discharge in 1 M $LiPF_6$ in PC saturated with O_2 are reported in Figure 3. There is no evidence of any Li_2O_2, but a band associated with Li_2CO_3 is apparent. We conclude that no significant quantity of Li_2O_2 can be detected on discharge.

3.2. The Charging Process. Although the recently reported MS data on charging an organic carbonate Li−O_2 cell after the

dx.doi.org/10.1021/ja2021747 |J. Am. Chem. Soc. 2011, 133, 8040–8047

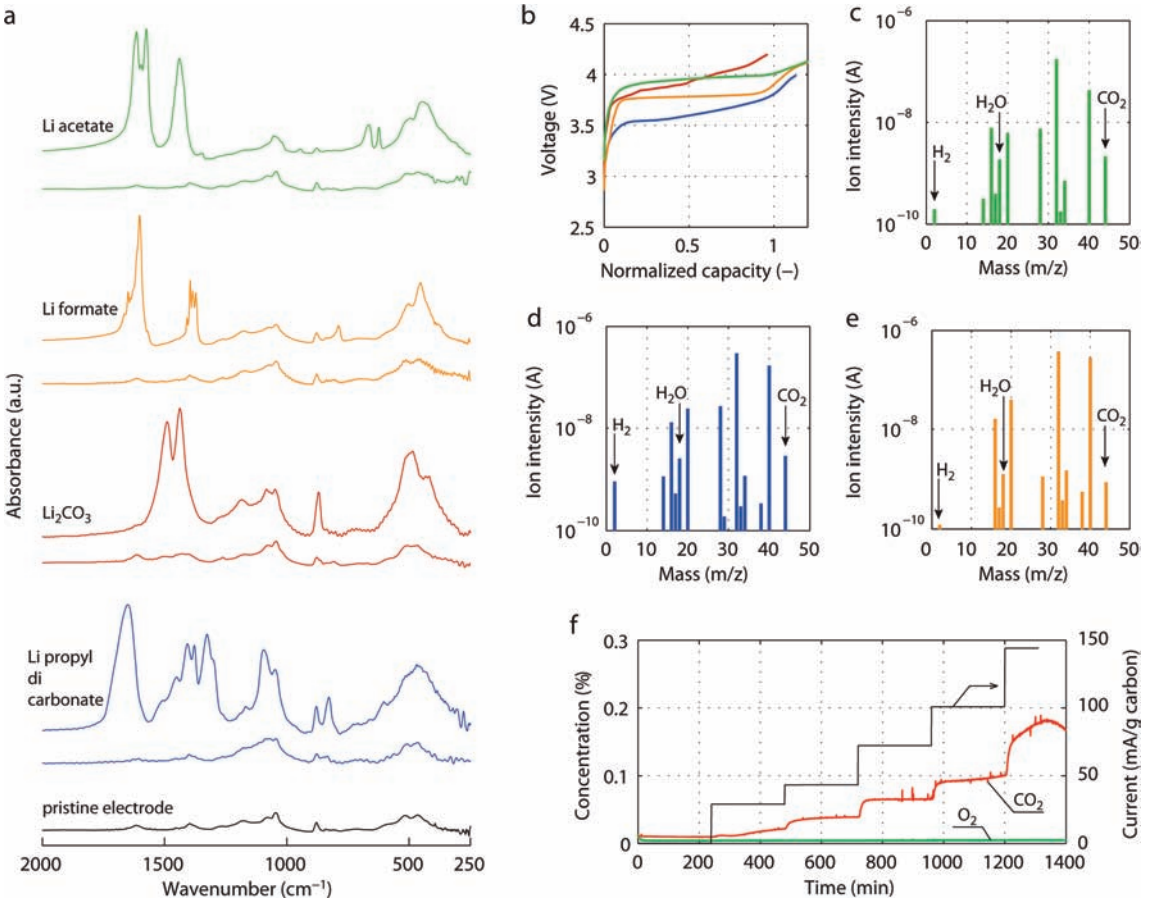

Figure 5. Composite electrodes (Super P/α-MnO_2/Kynar) that contain the discharge products individually were subjected to charging in 1 M $LiPF_6$ in PC under O_2. (a) FTIR spectra of the as-prepared electrodes and the charged electrodes for each of the compounds, together with the spectrum of a pristine electrode. (b) The corresponding charging curves at 70 mA/g (based on mass of carbon). Since the theoretical capacities of the different compounds vary, to aid comparison the capacities are all normalized to unity (theoretical capacities: Li propyl dicarbonate 1000 mA h/g, 2 e^-/mol; Li_2CO_3 1500 mA h/g, 2e^-/mol; CH_3CO_2Li 750 mA h/g, 1e^-/mol; HCO_2Li 750 mA h/g, 1e^-/mol). (c–e) MS gas analysis at the end of charging under O_2 of CH_3CO_2Li (c), $C_3H_6(OCO_2Li)_2$ (d), and HCO_2Li (e). Note that unmarked peaks arise from fragments of CO_2, H_2O, O_2, and Ar. (f) Gas evolution measured by DEMS on oxidation of a composite electrode containing Li_2CO_3 in response to a stepwise increased current under Ar.

first discharge demonstrated CO_2 evolution, suggesting decomposition of carbonates,[31] it did not provide direct evidence of carbonate decomposition and in particular did not report how the different discharge products decompose on charging. Here we examine how each of the discharge products behaves on charge using a combination of DEMS, MS, FTIR, and PXRD.

Before considering each product separately, FTIR spectra were collected on a pristine composite electrode, an electrode after discharge, and then subsequent charge, Figure 4. The spectra from the pristine electrode and the electrode after one cycle are identical, indicating that the products formed on discharge are decomposed on charging. Composite electrodes containing each of the discharge products separately were prepared and charged, Figure 5. The FTIR spectra in Figure 5a confirm the decomposition of each compound on charging. The charging voltages for Li_2CO_3, HCO_2Li, and CH_3CO_2Li are in a similar range, close to the charging voltage of the cell in Figure 4; the charging voltage of $C_3H_6(OCO_2Li)_2$ is somewhat lower, Figure 5b. As a result, when $C_3H_6(OCO_2Li)_2$ is present in the mixture of discharge products, it is subjected to a higher overpotential on charging, Figure 4b. Possible mechanisms for decomposition of $C_3H_6(OCO_2Li)_2$, Li_2CO_3, CH_3CO_2Li, and HCO_2Li on charging are described below and presented in Scheme 2.

3.2.1. $C_3H_6(OCO_2Li)_2$. The charging mechanism for $C_3H_6(OCO_2Li)_2$, Scheme 2, involves oxidation of the two terminal carbonate groups to yield an ·ORO· diradical, **5**, which can react in two ways. It can either undergo oxidative decomposition reactions in the presence of O_2 to yield CO_2 and H_2O, reaction 10, or abstract a proton (e.g., from H_2O) to form propylene glycol, reaction 11.[45] The proposed reaction scheme is consistent with the MS analysis on charging, Figure 5d, which shows evolution of CO_2 and H_2O; it is also in accord with the amount of CO_2 evolved, Table 1. If oxidation involved decomposition of **5** only via reaction 11, then 2 mol of CO_2 per mol of $C_3H_6(OCO_2Li)_2$ is predicted; if reaction 10 also occurs, then additional CO_2 is predicted. Experimentally, Table 1, 2.3 mol of CO_2 is observed, indicating both paths occur. The formation of propylene glycol on charging $C_3H_6(OCO_2Li)_2$ was demonstrated as follows. An electrode containing $C_3H_6(OCO_2Li)_2$ was charged in 1 M $LiPF_6$ in tri-ethylene glycol dimethyl ether. A thick gel formed on the Li metal anode, which was scraped off at the end of charging, washed with CH_3CN, and analyzed by ^1H NMR in D_2O, see Figure S5. Propylene glycol was detected along

dx.doi.org/10.1021/ja2021747 |*J. Am. Chem. Soc.* 2011, 133, 8040–8047

Scheme 2. Proposed Mechanisms of Charging $C_3H_6(OCO_2Li)_2$, Li_2CO_3, HCO_2Li, and CH_3CO_2Li

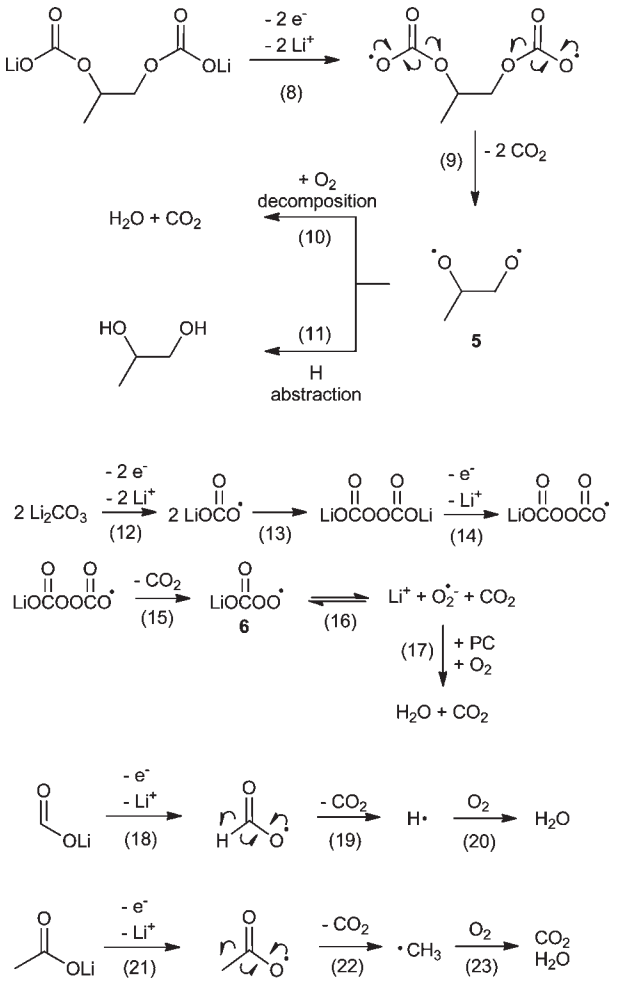

Table 1. Moles of CO_2 Evolved per Mole of Compound on Oxidation (charging)[a]

	mol CO_2/mol compound	
compound	theoretical	experimental
$C_3H_6(OCO_2Li)_2$	≥2	2.3 ± 0.12
Li_2CO_3	≥1	1.7 ± 0.05
HCO_2Li	1	0.9 ± 0.05
CH_3CO_2Li	2	2.0 ± 0.14

[a] Theoretical values are based on the reactions in Scheme 2; experimental values are obtained from the MS analysis of gas evolution on charge, Figure 5.

with some remaining ether. The process can be understood as follows. Oxidation of $C_3H_6(OCO_2Li)_2$ produces propylene glycol, Scheme 2. The gel then forms from the direct reduction of the propylene glycol on the Li surface, resulting in products such as Li propoxide, which can account for part of the H_2 evolution, Figure 5d. On washing the gel with D_2O, this converts back to propylene glycol. Tri-ethylene glycol dimethyl ether was chosen for the electrolyte to avoid possible confusion between the products of $C_3H_6(OCO_2Li)_2$ oxidation and products that

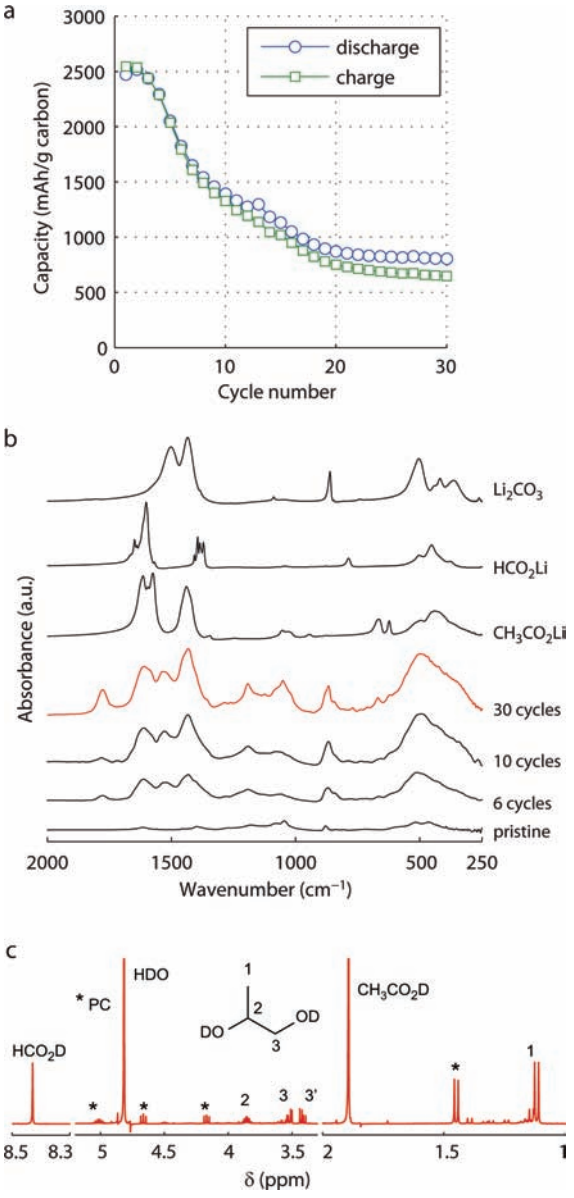

Figure 6. (a) Discharge and charge capacity vs cycle number for a composite electrode (Super P/α-MnO_2/Kynar) cycled between 2 and 4.2 V in 1 M $LiPF_6$ in PC under O_2. (b) FTIR spectra of composite electrodes. Pristine and after the indicated number of cycles between 2 and 4.2 V at the end of charge. Spectra of Li acetate, formate, and carbonate are shown for comparison. (c) ^1H solution NMR spectrum of D_2O extract from the composite electrode after 30 cycles at the end of charge. Integration of the areas under the peaks yields a mole ratio of Li propyl dicarbonate/Li acetate/Li formate of 1:3:1.1 (corresponding to a mass ratio of 1:1.09:0.32).

could form by direct contact between Li and PC electrolyte. We have observed large amounts of a gel-like substance on the Li metal anode on cycling many Li−O_2 cells with PC electrolytes, which far exceeds the usual SEI layer formation.[36,49]

3.2.2. Li_2CO_3. Since Li_2CO_3 is readily detected by powder X-ray diffraction, such data were collected before and after charging, Figure S6, confirming the disappearance of the Li_2CO_3 in accord with the FTIR data, Figure 5a. To investigate the oxidation of Li_2CO_3 DEMS data were collected during charging under Ar, Figure 5f, in order to probe possible O_2 evolution;

dx.doi.org/10.1021/ja2021747 |J. Am. Chem. Soc. 2011, 133, 8040–8047

CO_2 was evolved, but there is almost no O_2. Charging was also carried out under O_2, and the MS results showed that the only additional gases were CO_2, H_2O, and H_2. Previous studies of carbonate oxidation in aqueous solutions have described a mechanism involving peroxydicarbonate as an intermediate.[50] A similar mechanism is proposed in Scheme 2 and is consistent with the evolution of CO_2 but not O_2, as observed. After formation of the peroxydicarbonate by $1e^-$ oxidation and dimerization, reactions 12 + 13,[50] further oxidation and decarboxylation, reactions 14 + 15, can yield the $CO_4\cdot^-$ radical **6**. The equilibrium, reaction 16, between the radical **6** and $CO_2 + O_2^-$ has been described previously.[47] The O_2^- will in turn react with, e.g., PC to evolve additional CO_2 rather than being oxidized to dioxygen.[34] Together, these data demonstrate that it is indeed possible to charge, and hence decompose, Li_2CO_3 within the voltage range studied here. Analysis of the gases evolved on charging under O_2 show that 1.7 mol of CO_2 per mol Li_2CO_3 is obtained, in accord with the mechanism in Scheme 2.

3.2.3. HCO_2Li and CH_3CO_2Li. After removal of one electron and loss of CO_2, then H· and $\cdot CH_3$ radicals can form, respectively. In the presence of O_2 they may react to produce $HO_2\cdot$ and $CH_3OO\cdot$, which then further decompose to H_2O and CO_2, in accord with previous studies.[45,51] This is supported by mass spectra of the gas phase after charging HCO_2Li and CH_3CO_2Li in O_2, which show H_2 and H_2O evolution along with CO_2, Figure 5c+e. The close match between the amount of CO_2 predicted to be evolved based on Scheme 2 and the observed CO_2 evolution, Table 1, supports the proposed reaction paths. Again, H_2 can arise by reaction of evolved H_2O with the Li metal anode.

3.3. Cycling and Capacity Fading. Not only is it possible to recharge the Li−O_2 cell, even in the absence of reversible oxygen reduction to Li_2O_2, it is also possible to cycle the cell. Cycling involves, on discharge, repeated decomposition of the electrolyte and, on charge, oxidation of the decomposition products; however, why does the capacity fade on cycling? One obvious mechanism is electrolyte starvation: when the entire electrolyte is consumed, then discharge, and hence cycling, cannot take place. However fading and cell failure can occur even when there is ample electrolyte present. To investigate this question, a series of FTIR spectra were collected as a function of cycle number and at the end of charge; the data are presented in Figure 6b, along with the specific capacity as a function of cycle number. The FTIR spectrum at the end of charge after two cycles is identical to the as-prepared electrode; however, after six cycles, prominent bands at 1430 and 1530 cm^{-1} appear, and the band at 1610 cm^{-1} grows significantly in relative intensity. Associated with the changes in the FTIR spectra, a significant decrease in the specific capacity is observed, Figure 6a. After 10 and 30 cycles the changes in the FTIR become even more prominent, and the capacity continues to fade. The FTIR data indicate the accumulation of Li_2CO_3 and suggest the increasing presence of Li acetate and Li formate. To probe the products that accumulate on cycling further, a ^1H solution NMR spectrum of the D_2O extract from an electrode after 30 cycles at the end of charge was obtained, Figure 6c. Peaks indicate that the charged electrode after 30 cycles contains Li propyl dicarbonate, Li acetate, and Li formate in the ratios 1:3:1.1 (corresponding to a mass ratio of 1:1.09:0.32), along with the Li_2CO_3 clearly identified by FTIR. The relative proportions of Li acetate and Li formate are much higher than in the cathode after the first discharge where the ratios of Li propyl dicarbonate/Li acetate/Li formate were 1:0.22:0.21 (corresponding to a mass ratio of 1:0.084:0.062). This is why the acetate and formate can be clearly seen in the FTIR in Figure 6 but not in Figure 1. It appears that the capacity fading of the Li−O_2 cell with organic carbonate electrolyte is associated with the accumulation of these products in the cathode. PC also becomes increasingly trapped on cycling, as evident from the growing band at 1780 cm^{-1}, Figure 6b, and the NMR data, Figure 6c.

4. CONCLUSIONS

In conclusion, we have shown that the Li−O_2 cell, containing alkyl carbonate electrolyte, cycles by the decomposition of the electrolyte on discharge to form Li_2CO_3, $C_3H_6(OCO_2Li)_2$, CH_3CO_2Li, HCO_2Li, CO_2, and H_2O and oxidation of Li_2CO_3, $C_3H_6(OCO_2Li)_2$, CH_3CO_2Li, HCO_2Li on charging, with no evidence of reversible oxygen reduction to Li_2O_2. These reactions are not reversible, since the pathways for reduction (discharge) are different from oxidation (charge), correlating with the widely observed voltage gap (charging voltage greater than discharge even at low rates) in Li−O_2 cells. Oxidation of $C_3H_6(OCO_2Li)_2$ occurs at the terminal carbonate groups, leaving behind the OC_3H_6O moiety that reacts to form a thick gel-like deposit on the Li anode. Li_2CO_3, $C_3H_6(OCO_2Li)_2$, CH_3CO_2Li, and HCO_2-Li, accumulate in the cathode on cycling, resulting in capacity fading and eventually cell failure. Such a failure mechanism is compounded by consumption of the electrolyte on each cycle. Recog-
nition that organic carbonates are not suitable as electrolytes for Li−O_2 cells has led to interest in other solvents. Ethers are attractive because they can function with Li anodes, are of low cost, and are safe; however, we shall show in a future paper that, although more stable than carbonates, they too exhibit decomposition of the electrolyte. Successful Li_2O_2 formation/decomposition has been demonstrated in acetonitrile,[52] but this is not a suitable solvent for practical lithium cells, especially with Li metal anodes.

■ ASSOCIATED CONTENT

Supporting Information. Experimental procedures, supporting figures, and reaction schemes. This material is available free of charge via the Internet at http://pubs.acs.org.

■ AUTHOR INFORMATION

Corresponding Author
p.g.bruce@st-andrews.ac.uk

■ ACKNOWLEDGMENT

P.G.B. is indebted to the EPSRC, EU, and Toyota Motor Europe for financial support.

■ REFERENCES

(1) Abraham, K. M.; Jiang, Z. *J. Electrochem. Soc.* **1996**, *143*, 1.
(2) Read, J. *J. Electrochem. Soc.* **2002**, *149*, A1190.
(3) Read, J.; Mutolo, K.; Ervin, M.; Behl, W.; Wolfenstine, J.; Driedger, A.; Foster, D. *J. Electrochem. Soc.* **2003**, *150*, A1351.
(4) Ogasawara, T.; Debart, A.; Holzapfel, M.; Novak, P.; Bruce, P. G. *J. Am. Chem. Soc.* **2006**, *128*, 1390.
(5) Kuboki, T.; Okuyama, T.; Ohsaki, T.; Takami, N. *J. Power Sources* **2005**, *146*, 766.

(6) Visco, S. J.; Katz, B. D.; Nimon, Y. S.; De Jonghe, L. C.; U.S. Patent 7,011,7007, 2007.
(7) Imanishi, N.; Hasegawa, S.; Zhang, T.; Hirano, A.; Takeda, Y.; Yamamoto, O. *J. Power Sources* **2008**, *185*, 1392.
(8) Débart, A.; Paterson, A.; Bao, J.; Bruce, P. *Angew. Chem., Int. Ed.* **2008**, *47*, 4521.
(9) Yang, X.-H.; He, P.; Xia, Y.-Y. *Electrochem. Commun.* **2009**, *11*, 1127.
(10) Beattie, S. D.; Manolescu, D. M.; Blair, S. L. *J. Electrochem. Soc.* **2009**, *156*, A44.
(11) Laoire, C. O.; Mukerjee, S.; Abraham, K. M.; Plichta, E. J.; Hendrickson, M. A. *J. Phys. Chem. C* **2009**, *113*, 20127.
(12) Laoire, C. O.; Mukerjee, S.; Abraham, K. M.; Plichta, E. J.; Hendrickson, M. A. *J. Phys. Chem. C* **2010**, *114*, 9178.
(13) Wang, Y.; Zhou, H. *J. Power Sources* **2010**, *195*, 358.
(14) Kumar, B.; Kumar, J.; Leese, R.; Fellner, J. P.; Rodrigues, S. J.; Abraham, K. M. *J. Electrochem. Soc.* **2010**, *157*, A50.
(15) Hummelshoj, J. S.; Blomqvist, J.; Datta, S.; Vegge, T.; Rossmeisl, J.; Thygesen, K. S.; Luntz, A. C.; Jacobsen, K. W.; Norskov, J. K. *J. Chem. Phys.* **2010**, *132*, 071101.
(16) Bryantsev, V. S.; Blanco, M.; Faglioni, F. *J. Phys. Chem. A* **2010**, *114*, 8165.
(17) Lu, Y.-C.; Xu, Z.; Gasteiger, H. A.; Chen, S.; Hamad-Schifferli, K.; Shao-Horn, Y. *J. Am. Chem. Soc.* **2010**, *132*, 12170.
(18) Xu, W.; Xiao, J.; Wang, D.; Zhang, J.; Zhang, J.-G. *Electrochem. Solid-State Lett.* **2010**, *13*, A48.
(19) Mohamed, S. N.; Johari, N. A.; Ali, A. M. M.; Harun, M. K.; Yahya, M. Z. A. *J. Power Sources* **2008**, *183*, 351.
(20) Lu, Y.-C.; Gasteiger, H. A.; Crumlin, E.; Robert McGuire, J.; Shao-Horn, Y. *J. Electrochem. Soc.* **2010**, *157*, A1016.
(21) Lu, Y.-C.; Gasteiger, H. A.; Parent, M. C.; Chiloyan, V.; Shao-Horn, Y. *Electrochem. Solid-State Lett.* **2010**, *13*, A69.
(22) Peled, E.; Golodnitsky, D.; Mazor, H.; Goor, M.; Avshalomov, S. *J. Power Sources* 10.1016/j.jpowsour.2010.09.104.
(23) Aleshin, G. Y.; Semenenko, D. A.; Belova, A. I.; Zakharchenko, T. K.; Itkis, D. M.; Goodilin, E. A.; Tretyakov, Y. D. *Solid State Ionics* **2011**, *184*, 62.
(24) Cheng, H.; Scott, K. *J. Power Sources* **2010**, *195*, 1370.
(25) Zhang, S. S.; Foster, D.; Read, J. *J. Power Sources* **2010**, *195*, 1235.
(26) Zhang, D.; Fu, Z.; Wei, Z.; Huang, T.; Yu, A. *J. Electrochem. Soc.* **2010**, *157*, A362.
(27) Andrei, P.; Zheng, J. P.; Hendrickson, M.; Plichta, E. J. *J. Electrochem. Soc.* **2010**, *157*, A1287.
(28) Mizuno, F.; Nakanishi, S.; Kotani, Y.; Yokoishi, S.; Iba, H. *Electrochemistry* **2010**, *78*, 403.
(29) Freunberger, S. A.; Hardwick, L. J.; Peng, Z.; Giordani, V.; Chen, Y.; Maire, P.; Novák, P.; Tarascon, J.-M.; Bruce, P. G. In *IMLB 2010* ; 15th International Meeting on Lithium Batteries, Montreal, Canada,June 27 to July 2, 2010.
(30) Freunberger, S. A.; Peng, Z.; Hardwick, L. J.; Chen, Y.; Barde, F.; Bruce, P. *ECS Meet. Abstr.* **2010**, *1002*, 340.
(31) Xu, W.; Viswanathan, V. V.; Wang, D.; Towne, S. A.; Xiao, J.; Nie, Z.; Hu, D.; Zhang, J.-G. *J. Power Sources* **2011**, *196*, 3894.
(32) Dobley, A.; Morein, C.; Abraham, K. M. *ECS Meet. Abstr.* **2006**, *502*, 823.
(33) Ufheil, J.; Wursig, A.; Schneider, O. D.; Novak, P. *Electrochem. Commun.* **2005**, *7*, 1380.
(34) Aurbach, D.; Daroux, M.; Faguy, P.; Yeager, E. *J. Electroanal. Chem.* **1991**, *297*, 225.
(35) Gibian, M. J.; Sawyer, D. T.; Ungermann, T.; Tangpoonpholvivat, R.; Morrison, M. M. *J. Am. Chem. Soc.* **1979**, *101*, 640.
(36) Aurbach, D.; Daroux, M. L.; Faguy, P. W.; Yeager, E. *J. Electrochem. Soc.* **1987**, *134*, 1611.
(37) Fong, R.; Reid, M. C.; McMillan, R. S.; Dahn, J. R. *J. Electrochem. Soc.* **1987**, *134*, 516.
(38) Aurbach, D.; Gofer, Y.; Langzam, J. *J. Electrochem. Soc.* **1989**, *136*, 3198.
(39) San Filippo, J.; Romano, L. J.; Chern, C.-I.; Valentine, J. S. *J. Org. Chem.* **1976**, *41*, 586.
(40) Bryantsev, V. S.; Blanco, M. *J. Phys. Chem. Lett.* **2011**, 379.
(41) McDonald, R. N.; Chowdhury, A. K. *J. Am. Chem. Soc.* **1985**, *107*, 4123.
(42) Behrendt, W.; Gattow, G.; Draeger, M. *Z. Anorg. Allg. Chem.* **1973**, *397*, 237.
(43) Matsumoto, S.; Sugimoto, H.; Sawyer, D. T. *Chem. Res. Toxicol.* **1988**, *1*, 19.
(44) Curran, H. J.; Gaffuri, P.; Pitz, W. J.; Westbrook, C. K. *Combust. Flame* **1998**, *114*, 149.
(45) Atkinson, R. *Int. J. Chem. Kinet.* **1997**, *29*, 99.
(46) Sinha, A.; Thomson, M. J. *Combust. Flame* **2004**, *136*, 548.
(47) Roberts, J. L.; Calderwood, T. S.; Sawyer, D. T. *J. Am. Chem. Soc.* **1984**, *106*, 4667.
(48) Wadhawan, J. D.; Welford, P. J.; Maisonhaute, E.; Climent, V.; Lawrence, N. S.; Compton, R. G.; McPeak, H. B.; Hahn, C. E. W. *J. Phys. Chem. B* **2001**, *105*, 10659.
(49) Verma, P.; Maire, P.; Novák, P. *Electrochim. Acta* **2010**, *55*, 6332.
(50) Zhang, J.; Oloman, C. W. *J. Appl. Electrochem.* **2005**, *35*, 945.
(51) Chin, D. H.; Chiericato, G.; Nanni, E. J.; Sawyer, D. T. *J. Am. Chem. Soc.* **1982**, *104*, 1296.
(52) Peng, Z.; Freunberger, S. A.; Hardwick, L. J.; Chen, Y.; Giordani, V.; Bardé, F.; Novák, P.; Graham, D.; Tarascon, J.-M.; Bruce, P. G. *Angew. Chem., Int. Ed.* **2011**; accepted.